Food Hydrocolloids 70 (2017) 363–370

Contents lists available at ScienceDirect

Food Hydrocolloids

journal homepage: www.elsevier.com/locate/foodhyd

Biopolymer nanoparticles for vehiculization and photochemical stability preservation of retinol

Flavia F. Visentini [a, b], Osvaldo E. Sponton [a, b], Adrián A. Perez [a, b], Liliana G. Santiago [b, *]

[a] Consejo Nacional de Investigaciones Científicas y Técnicas de la República Argentina, CONICET, Argentina
[b] Área de Biocoloides y Nanotecnología, Instituto de Tecnología de Alimentos, Facultad de Ingeniería Química, Universidad Nacional del Litoral, 1 de Mayo 3250, Santa Fe 3000, Argentina

ARTICLE INFO

Article history:
Received 30 December 2016
Received in revised form
15 April 2017
Accepted 15 April 2017
Available online 18 April 2017

Keywords:
Retinol
Ovalbumin
Heat-induced nanoparticle
High methoxyl pectin
Biopolymer nanoparticle
Photochemical stability

ABSTRACT

This paper gives experimental information about the production of biopolymer nanoparticles (BNPs) for vehiculization and photochemical preservation of retinol (RET). BNPs production involved the combination of two biopolymer functional properties: (i) protein ability for binding RET, in order to form protein-RET nanocomplexes, and (ii) polysaccharide deposition onto the protein-RET nanocomplexes surface so as to obtain BNPs. A particular set of biopolymer materials was employed: native ovalbumin (OVA), OVA nanosized aggregate (OVAn) and high methoxyl pectin (HMP). Absorbance, particle size distribution and ζ potential measurements, suggested OVA aggregation mainly influenced the production of colloidal stable BNPs. At protein:HMP ratio ($R_{Prot:HMP}$) 2:1, the most appropriated pH values for obtaining BNPs were: 4.0 for OVA-HMP system, and 6.0 for OVAn-HMP system. RET photochemical decomposition in BNPs was examined over 30 h. It was observed that HMP deposition on protein-RET nanocomplex surface improved the RET photochemical stability. OVAn-RET-HMP nanoparticle formed at pH 6.0 promoted a lower RET photochemical decomposition (14.1%) in comparison with the one registered for OVA-RET-HMP nanoparticle formed at pH 4.0 (25.0%). Because of denatured/aggregated state, the OVAn particular features to bind RET and to interact with HMP could explain the observed BNPs performance. Information derived from this work could be extrapolated for vehiculization and protection of other photosensitive lipophilic compounds.

1. Introduction

Protein-polysaccharide interactions find several applications in a lot of research and development sectors, e.g. food, pharmaceutics, cosmetics, etc. In food industry, these interactions had been widely exploited for enhancement of biopolymer functionality in complex food, and for the obtention of supramolecular structures so as to control texture and stability of colloidal dispersed systems (Fioramonti, Martínez, Pilosof, Rubiolo, & Santiago, 2015; Perez, Carrera Sánchez, Rodríguez Patino, Rubiolo, & Santiago, 2012). More recently, studies about biopolymer interactions have been focused on the creation of biopolymer nanoparticles (BNPs) which can be used as delivery systems for vehiculization and protection of bioactive compounds (Fioramonti, Perez, Aringoli, Rubiolo, & Santiago, 2014; Noshad, Mohebbi, Shahidi, & Koocheki, 2015; Perez, Sponton, Andermatten, Rubiolo, & Santiago, 2015; Zhang et al., 2015). This challenge involves to know aqueous medium conditions (e.g. pH, ionic strength, biopolymer relative concentration, cosolutes presence) which promote the appropriate biopolymer self-assembly (Chanasattru, Jones, Decker, & McClements, 2009; Li & McClements, 2013; Qiu et al., 2017; Zeeb, Stenger, Hinrichs, & Weiss, 2016). This phenomenon is governed by different intermolecular forces, e.g. electrostatic, hydrophobic, van der Waals, hydrogen point, etc., which occur under certain environmental conditions in close relationship with physicochemical features of involved macromolecules. In nanotechnology field, the strategy employing biopolymer self-assembly principles is named *bottom-up* technology, being this one a powerful tool to obtain tailor-made particles with defined sizes, surface and delivery properties (Chen, Remondetto, & Subirade, 2006; Jones & McClements, 2010; Joye & McClements, 2014; Lesmes & McClements, 2009). BNPs for lipophilic bioactive compound delivery can be designed by applying the following functional properties:

* Corresponding author.
E-mail address: lsanti@fiq.unl.edu.ar (L.G. Santiago).

http://dx.doi.org/10.1016/j.foodhyd.2017.04.020
0268-005X/

(i) Ligand binding to protein for obtaining inclusion complexes (Joye & McClements, 2014; Perez, Andermatten, Rubiolo, & Santiago, 2014; Visentini, Sponton, Perez, & Santiago, 2016). Hydrophobic forces at specific protein domains mainly conduct molecular binding, which usually promote the ligand solubilization in aqueous medium. Besides, lipophilic ligand binding can be increased if protein conformation is altered by denaturation/aggregation process, e.g. controlled heat treatment (Sponton, Perez, Carrara, & Santiago, 2015a). In this case, a greater protein surface hydrophobicity could favor an increased ligand loading capacity per inclusion complex unit (Sponton, Perez, Carrara, & Santiago, 2016).

(ii) Polysaccharide deposition onto the inclusion complex surface (Perez et al., 2015). Electrostatic forces mainly govern this phenomenon, depending on polysaccharide chemical nature and protein conformational state (Fioramonti et al., 2014). In some cases, this leads to a cover formation which promote ligand protection against several injurious environmental factors (Perez et al., 2015; Zimet & Livney, 2009).

In this framework, the present paper is aimed to get experimental information about appropriate protein-polysaccharide interactions in order to produce BNPs for photosensitive compound delivery. The research especially emphasized on the production of nanosized particles with high colloidal stability in aqueous formulations. In concordance with previous studies, a particular set of materials was employed: native ovalbumin (OVA), OVA nanosized aggregate (OVAn) formerly characterized in our lab, retinol (RET) as a model of photosensitive lipophilic compound, and high methoxyl pectin (HMP) as anionic polysaccharide. OVA is a monomeric protein of 43 KDa, and it has 4 sulfhydryl groups (−SH) and one disulfide bond (S−S) per monomer (Weijers & Visschers, 2002). It is constituted of 385 aminoacids, from which a half is hydrophobic and mainly buried into the protein structure and a third are charged aminoacids (Nisbet, Saundry, Moir, Fothergill, & Fothergill, 1981). The OVA properties for binding hydrophobic ligand have been poorly studied, so this globular protein could be evaluated in innovative binding studies. OVAn is a nanosized heat-induced aggregate with a great surface hydrophobicity, which it could enhance the ability for binding hydrophobic ligands (Sponton, Perez, Carrara, & Santiago, 2015b). Finally, as it was recently reported, HMP is able to produce an electrostatic deposition (cover) onto the surface of protein-ligand complexes leading a great protection against injurious factors (Perez et al., 2015). Moreover, it is worthy to remark that this contribution is continued from a previous work, in which OVA and OVAn were assayed for vehiculization and photochemical protection of RET (Visentini et al., 2016). Results highlighted that RET photochemical stability depended on aqueous medium pH and protein conformational state (native vs aggregated). Nevertheless, the hypothesis if a polysaccharide electrostatic cover could enhance RET photochemical stability via favorable interactions with OVA and OVAn, remained to be confirmed. The present paper will address this hypothesis.

2. Materials and methods

2.1. Materials

Native ovalbumin (OVA, product A5503, purity 98% according to agarose gel electrophoresis) was purchased from Sigma (USA). Ovalbumin nanosized aggregate (OVAn) was produced according to Sponton et al. (2015b). Briefly, OVA dispersion was prepared at 10 g/L, 50 mM NaCl and pH 7.5. Then, 2 mL aliquots were dispensed in glass tubes and were heated in a water bath at 85 °C for 5 min. Subsequently, tubes were removed and immediately cooled in an ice bath. Tubes containing OVAn were kept at 4 °C until further analysis. Retinol (RET; product 17772, purity ≥95.0% according to HPLC) was also obtained from Sigma (USA). RET was kept in darkness under N_2 atmosphere at −20 °C according to manufacturer advice. High methoxyl pectin (HMP) was kindly supplied by Cargill (Argentina) and had 68.0 ± 2.0% degree of esterification (DE). According to Cargill information, composition (wt.%), was: 87.0% carbohydrate, 11.0% moisture, and 2.0% ash (Na^+ 480 mg/100 g and K^+ 160 mg/100 g, Ca^{+2} 200 mg/100 g, Mg^{+2} 30 mg/100 g and Fe^{+2} 2 mg/100 g).

2.2. Production of protein-retinol nanocomplexes

The obtention of OVA-RET and OVAn-RET nanocomplexes was performed according to Visentini et al. (2016). In summary, OVA and OVAn dispersions (23 μM) were prepared in phosphate buffer (pH 7, 50 mM). On the other hand, a 250 mM RET stock solution was prepared in ethanol. Then, protein (OVA or OVAn) dispersion and ethanolic RET solution were mixed so as to produce the saturation of protein binding sites. It is important to remark that final ethanol concentration in mixed systems was lower than 1 vol%; therefore, it could be assumed that no protein structural modifications were induced (Cogan, Kopelman, & Shinitzky, 1976). Protein-RET nanocomplexes dispersions were stored in darkness for 2 h for reaching equilibrium.

2.3. Obtention of protein-polysaccharide nanoparticles

Strategy used for biopolymer nanoparticles (BNPs) obtention involved the combination of two functional properties: (i) proteins (OVA and OVAn) ability for binding RET, in order to obtain protein-RET nanocomplexes, and (ii) HMP deposition onto the protein-RET nanocomplexes for obtaining BNPs. For this, a set for complementary techniques was applied. These ones are described as follows.

2.3.1. Biopolymer phase behaviour

In order to get information about protein-polysaccharide interactions promoting colloidally stable BNPs formation, a study of biopolymer phase behaviour was firstly performed. Biopolymer mixed systems (OVA-HMP and OVAn-HMP systems) were prepared at protein-polysaccharide concentration ratio ($R_{Prot:Ps}$) 2:1, according to Perez et al. (2015). For this, proteins (OVA and OVAn) and HMP dispersions were prepared in phosphate buffer pH 7.0. HMP dispersion was previously heated at 70 °C for 15 min for promoting the adequate polysaccharide hydration. In all systems protein concentration was 23 μM (0.1 wt.%, protein concentration used for RET-protein complexes obtention) and HMP concentration was 0.05 wt.%. Mixed systems were obtained by mixing the appropriate volume of each double concentrated biopolymer solution up to the final required bulk concentration. The phase behaviour in aqueous dispersions was evaluated considering two experimental approaches: (i) absorbance (ABS) measurements at 400 nm, and (ii) visual appearance of biopolymer systems at 24 h after preparation. For this, biopolymers mixed systems were prepared at different pH values from 7.0 to 2.5. The pH was adjusted by using 1 M HCl solution. ABS was determined as soon as systems were prepared, using a Jenway 7305 spectrophotometer (UK). ABS values were interpreted as a measure of biopolymer molecular size and/or the number of biopolymer absorbent entities (Perez et al., 2015). Subsequently, the biopolymer mixed systems at different pH values were kept in repose at room temperature (25 °C) for 24 h, and their visual appearances were registered by means of a photo camera (Cyber-shot 12.1 mpx, Sony, USA). According the phase behaviour

results, the most appropriated pH values for soluble BNPs formation were selected.

2.3.2. Particle size distribution and ζ potential analysis

The effect of RET complexation on particle size and electrical properties for BNPs was examined by means of particle size distribution (PSD) and ζ potential analysis. For this, a Zetasizer Nano ZS90 (Malvern Instruments Ltd., UK) equipment was employed. PSD was obtained by dynamic light scattering (DLS) at 90° and at 632.8 nm wavelength. Particle hydrodynamic diameter (d_H) was obtained from the intensity (%) distribution (PSDi). PSD in volume (%, PSDv) was also considered in particle diameter analysis. PSDv was generated from PSDi by applying Mie theory. The ζ potential measurements were determined from electrophoretic mobility distribution of particles by means of laser Doppler velocity technique. The ζ potential values were calculated according to Smoluchowski model (Hunter, 2001), by using the equipment software. All determinations were performed in duplicate at 25 °C.

2.4. Determination of retinol photochemical decomposition

The RET photochemical decomposition in BNPs aqueous dispersions was evaluated according to Shimoyamada, Yoshimura, Tomida, and Watanabe (1996), and it was determined as a percentage of the initial ABS at 330 nm (ABS_0) over 30 h. Thus, RET photochemical decomposition level was calculated as follows:

$$RET\ \ Decomposition\ \ (\%) = \frac{ABS_0 - ABS_t}{ABS_0} \times 100\% \qquad (1)$$

where ABS_t is ABS value at a given time in the range of 0–30 h. RET-protein and RET-protein-HMP systems were prepared as it was described in previous sections. In all systems, protein (OVA and OVAn), RET and HMP concentrations were: 6.7 μM (0.028 wt.%), 670 μM and 0.014% wt.%, respectively. The systems were placed at 35 cm (arbitrary position) under a compact fluorescent lamp (BAW, 65 W, 750 lm, 6400 K). Two kind of controls were also assayed: (i) pure RET solution kept in darkness, which was considered as a measure of RET photochemical decomposition due to dissolved oxygen (DO) in aqueous solution ($RET_{darkness}$), and (ii) pure RET solution kept under light exposition, which was considered as a measure of RET photochemical decomposition due to combined action of DO and light (RET_{light}). Experiments were conducted at room temperature (25 °C) in triplicate.

2.5. Dissolved oxygen determination

To get a better comprehension of results derived from RET photochemical decomposition assay, initial DO concentration was evaluated. DO was determined in systems without RET in order to know DO concentration at which RET would be initially exposed. Hence, the measurements were performed in phosphate buffer (included as control), and in the following systems: OVA at pH 4.0, OVA-HMP at pH 4 and at pH 6, OVAn at pH 6.0, and OVAn-HMP at pH 6. Standard iodometric test with azide modification was applied (Rice, Baird, Eaton, & Clesceri, 2012). Samples were placed in 250 mL Winkler frasks, 1 mL $MnSO_4$ solution was added, followed by 1 mL alkali-iodide-azide reagent. In order to exclude air bubbles, frasks were carefully capped and mixed by inverting a few times. Frasks remained in repose until precipitate was settled sufficiently. Then, 1 mL concentrated H_2SO_4 was added and mixed by inverting several times until dissolution was completed. A volume of 200 mL sample was titrated with 0.025 M $Na_2S_2O_3$ solution. Few drops of starch solution (as indicator) were added. Titration end point was considered at blue colour disappearance. For titration of 200 mL sample, 1 mL 0.025 M $Na_2S_2O_3$ is equivalent to 1 mg DO/L. Determinations were done at least in duplicate at room temperature (25 °C).

2.6. Statistical analysis

Statistical differences were determined through one-way analysis of variance (ANOVA) using StatGraphics Plus 3.0 software. For this, LSD test at 95% confidence level was applied.

3. Results and discussion

3.1. Phase behaviour of biopolymer mixed systems

The study of protein-polysaccharide interactions in aqueous solution would allow to know the experimental conditions in which colloidally stable BNPs for RET vehiculization are produced. Fig. 1 shows the pH-dependent phase behaviour for OVA-HMP and OVAn-HMP mixed systems. Phase behaviour was described in terms of ABS at 400 nm (Fig. 1A) and visual appearance of mixed systems (Fig. 1B and C). In this Fig., behaviour for pure OVA and OVAn dispersions was included as controls.

For OVA, ABS was practically zero over the whole pH range of assay, suggesting the small protein size. For OVA-HMP system, ABS was similar to the control up to pH around 4.5 from which ABS values abruptly increased reaching a maximum at pH 3.5–3.0. As it can be noted in Fig. 1B, mixed systems remained translucid up to pH

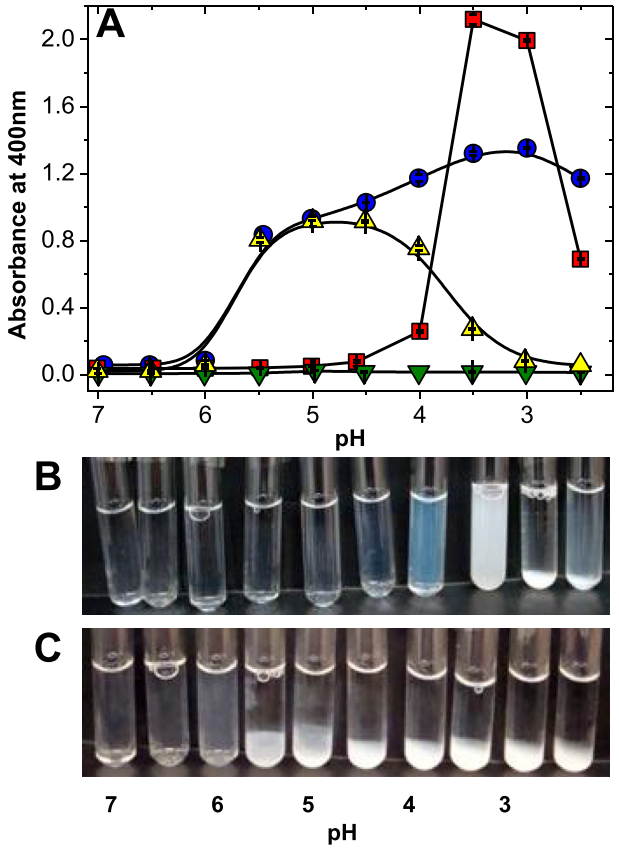

Fig. 1. Phase behaviour of pure proteins and protein-polysaccharide systems as a function of aqueous medium pH: ABS at 400 nm as a measure of system turbidity (A) for (▼) OVA, (■) OVA-HMP, (▲) OVAn and (●) OVAn-HMP and visual appearance for OVA-HMP (B) and for OVAn-HMP (C). Conditions: Protein concentration: 23 μM (0.1 wt.%), HMP concentration: 0.05 wt.%. Values in (A) are showed as mean ± standard deviation.

4.5 at 24 h examination. Furthermore, a decrease in aqueous medium pH caused the development of turbidity. At pH 4.0, it was registered an appreciable turbidity, suggesting the existence of bigger macromolecular species. Isoelectric point (pI) for OVA was pH ~4.7 (Visentini et al., 2016), and pKa value for HMP was assumed at 3.6, because of carboxylic group dissociation (Humblet-Hua Scheltens, van der Linden, & Sagis, 2011). So, at pH 4.0 attractive electrostatic interactions between OVA cationic groups and HMP anionic groups can be assumed. This fact could also be explained considering ζ potential values for OVA (+11 mV) and HMP (−27 mV) at pH 4.0, as it can be deduced from Table 1. These interactions resulted in the formation of soluble electrostatic complexes because system remained colloidally stable at long-term examination. Colloidal stability for OVA-HMP system is also reflected by their high ζ potential value (−23 mV), which could be strongly influenced by the polysaccharide anionic character. At pH 3.5, a great turbidity was observed (Fig. 1B) suggesting the presence of big electrostatic complexes. Then, a further decrease in pH promoted complex coacervation or associative phase separation, possibly due to the HMP negative charge neutralization, and the formation of precipitating biopolymer coacervates (Perez et al., 2015).

For OVAn, the decrease in pH caused a maximum ABS at pH 5.0–4.5 which could be explained by an increase in particle size due to the reduction in OVAn net charge. As it was reported by Visentini et al. (2016), pI for OVAn was estimated at ~ 4.7.

For OVAn-HMP system, it was noted ABS values were similar than the ones obtained for pure OVAn up to pH 5.0, from which ABS gradually increased until reach a maximum at pH 3.0. For this system, turbidity development was noted from pH 6.5 (Fig. 1C, as it can be also noted in Fig. 1A). Then, a decrease in aqueous medium pH caused an increase in turbidity. At pH 6.0, system remained colloidally stable, but a further decrease in pH caused phase separation. Table 1 shows ζ potential values for OVAn, HMP and OVAn-HMP system. It can be noted that both pure biopolymers are negatively charged (−18 mV for OVAn, and −28 mV for HMP). However, for OVAn-HMP system, it was registered ζ potential value −25 mV, which was significantly higher than the one for HMP ($p < 0.05$). In spite of at pH 6.0, repulsive interactions are predominant, some negative charge neutralization HMP by means of OVAn positive *patches* could occur. These weak associative interactions could lead to the formation of soluble complexes or hybrid supramolecular entities (Benichou, Aserin, Lutz, & Garti, 2007), and they could be particularly favored when protein conformation is altered by aggregation (Perez, Carrara, Carrera-Sánchez, Rodríguez-Patino, & Santiago, 2009). At pH between 6.0 and 5.0, phase separation could be explained by aggregation induced by a reduction of protein net charge, especially around OVAn pI. Below pH 5.0, strong attractive electrostatic interactions could promote the formation of protein-polysaccharide complexes and coacervates that precipitate as a consequence of their big sizes (Fioramonti et al., 2014).

According to these results, the more appropriate conditions to obtain BNPs for RET vehiculization are pH 4.0 and 6.0. Particles generated at these conditions were characterized in terms of their size and electrical properties, as it will be discussed in the next section.

3.2. Size and electrical properties of BNPs for RET vehiculization

In agro-food sector, definition of nanosized materials is still not clear. So, particles with both, size strictly <100 nm and with few hundred nm could be defined as “nanoparticles” (Gutiérrez et al., 2013; Joye, Davidov-Pardo, & McClements, 2014). In general, it is well established that small particle sizes and high ζ potentials are

Table 1
Effect of protein-RET and protein-RET-HMP complexation on ζ potential (mV), diameter (nm) and Volume (%) of OVA and OVAn as a function of aqueous medium pH. Conditions: Protein concentration: 23 μM (0.1 wt.%), RET concentration: 2.3 mM, HMP concentration: 0.05%. Temperature: 25 °C.

pH	Systems	Diameter (nm)	Volume (%)	ζ Potential (mV)
4.0	OVA	10 ± 1^{a} (peak 1)	92 ± 2	$+11 \pm 1^{g}$
		61 ± 2^{c} (peak 2)	8 ± 2	
	OVA-RET	203 ± 17^{d}	92 ± 1	$+12 \pm 0^{g}$
	OVA-HMP	253 ± 5^{f}	100 ± 0	-23 ± 0^{d}
	OVA-RET-HMP	286 ± 18^{g}	100 ± 0	-21 ± 1^{e}
	HMP[a]	990 ± 65^{k}	100 ± 0	-27 ± 0^{a}
6.0	OVA	9 ± 1^{a} (peak 1)	94 ± 0	-17 ± 1^{f}
		$52 \pm 2^{b,c}$ (peak 2)	6 ± 0	
	OVA-RET	239 ± 0^{e}	100 ± 0	-22 ± 1^{e}
	OVA-HMP	46 ± 4^{b} (peak 1)	88 ± 1	-28 ± 1^{a}
		535 ± 16^{j} (peak 2)	10 ± 2	
	OVA-RET-HMP	252 ± 6^{f}	96 ± 3	-27 ± 1^{b}
	OVAn	197 ± 3^{d}	98 ± 0	-18 ± 3^{f}
	OVAn-RET	353 ± 9^{h}	96 ± 1	-17 ± 0^{f}
	OVAn-HMP	231 ± 0^{e}	91 ± 4	-25 ± 1^{c}
	OVAn-RET-HMP	376 ± 10^{i}	99 ± 1	-23 ± 1^{d}
	HMP	–	–	-28 ± 1^{a}

Values are showed as mean ± standard deviation and different letters in each column indicate statistical differences ($p < 0.05$).
[a] Data taken from Perez et al. (2015).

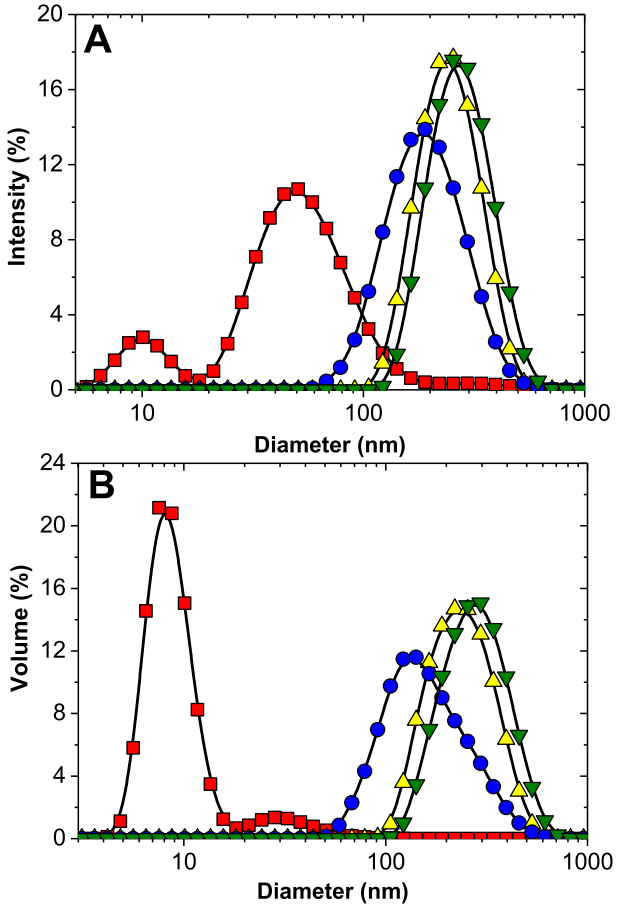

Fig. 2. Particle size distribution (PSD) based on Intensity and Volume percentage (%) at pH 4: (A) and (B): (■) OVA, (●) OVA-RET complex, (▲) OVA-HMP complex and (▼) OVA-RET-HMP complex. Conditions: Protein concentration: 23 μM (0.1 wt.%), RET concentration: 2.3 mM, HMP concentration: 0.05%. Temperature: 25 °C.

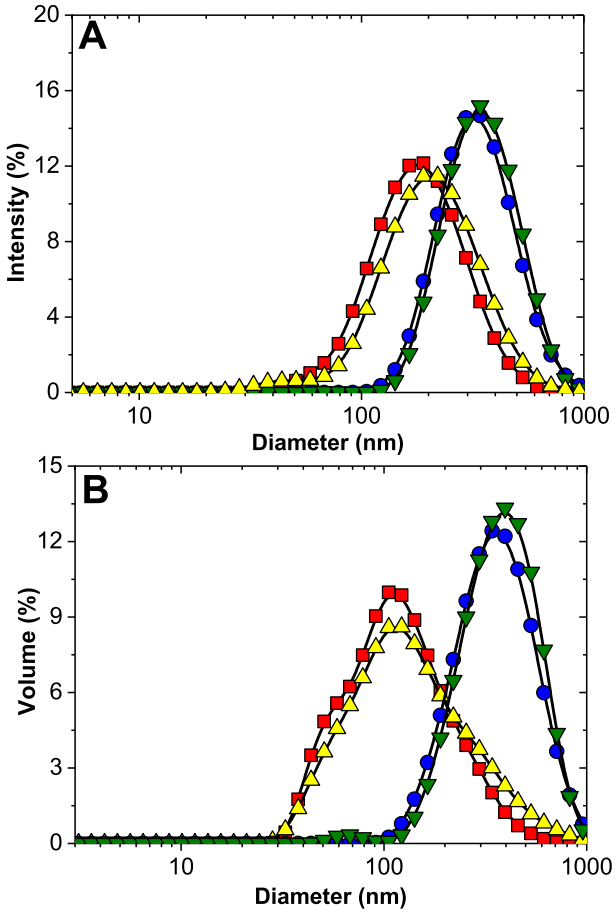

Fig. 3. Particle size distribution (PSD) based on Intensity and Volume percentage (%) at pH 6: (A) and (B): (■) OVAn, (●) OVAn-RET complex, (▲) OVAn-HMP complex and (▼) OVAn-RET-HMP complex. Conditions: Protein concentration: 23 μM (0.1 wt.%), RET concentration: 2.3 mM, HMP concentration: 0.05%. Temperature: 25 °C.

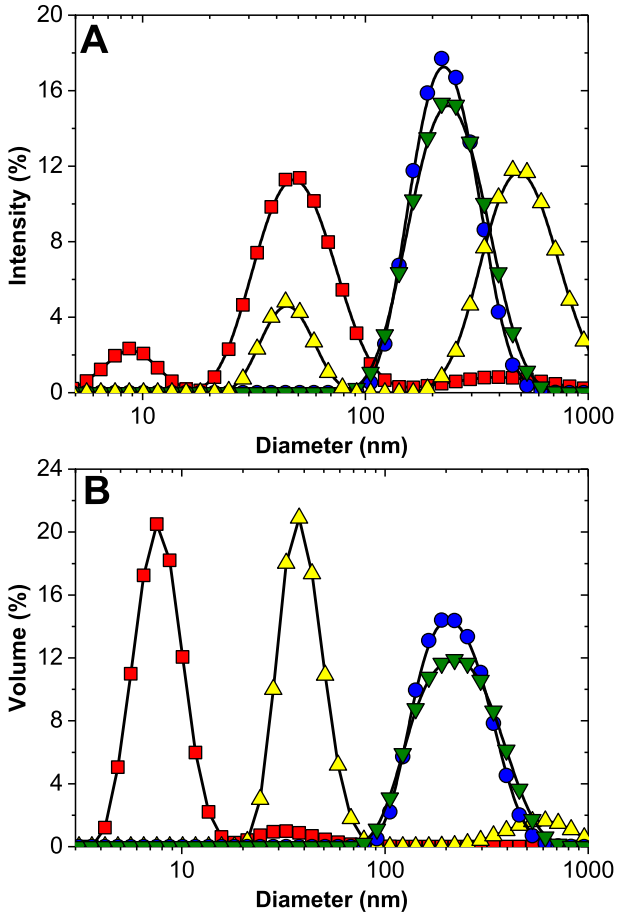

Fig. 4. Particle size distribution (PSD) based on Intensity and Volume percentage (%) at pH 6: (A) and (B): (■) OVA, (●) OVA-RET complex, (▲) OVA-HMP complex and (▼) OVA-RET-HMP complex. Conditions: Protein concentration: 23 μM (0.1 wt.%), RET concentration: 2.3 mM, HMP concentration: 0.05%. Temperature: 25 °C.

requirements needed to obtain a high colloidal stability in food aqueous mediums (Lesmes & McClements, 2009; Perez et al., 2015).

Figs. 2–4 shows the effect of RET binding (vehiculization) on the PSD for OVA-HMP and OVAn-HMP systems. For a better comprehension, PSD results are also shown in Table 1. Results are discussed as follows. At pH 4.0, for pure OVA, two peaks in PSDi at 10 ± 1 and 61 ± 2 nm were observed (Fig. 2A), representing 92 and 8%, respectively, as it was also deduced from PSDv (Fig. 4B). Visentini et al. (2016) reported the first peak would correspond to OVA hydrodynamic diameter (d_H), and the second one to traces of some aggregated protein. For OVA-RET complexes, an increase in OVA size (203 ± 17 nm, corresponding to 92%) after RET complexation was registered. In respect to this, it was also reported that one OVA monomeric unit is able to bind ~108 RET molecules with 10^5 M^{-1} affinity constant. Therefore, the increase in particle size for OVA-RET nanocomplex should be linked with the OVA ability for binding RET. As it was deduced from Table 1, at this pH value, RET complexation did not alter significantly the OVA ζ potential ($p > 0.05$), supporting the idea that colloidal stability of OVA-RET nanocomplex is mainly governed by OVA electrical properties.

In order to complete the BNPs formation, HMP deposition onto the surface of OVA-RET nanocomplex was performed at pH 4.0. It was noted that HMP deposition onto pure OVA surface caused BNP formation with d_H 253 ± 5 nm, corresponding to an intermediate particle size between OVA (10 ± 1 nm) and HMP (990 ± 65 nm), which highlighted the electrostatic self-assembly between biopolymers (Perez et al., 2015). As it was mentioned previously, ζ potential results for OVA, HMP and OVA-HMP systems support this result (Table 1). Besides, it was observed that RET binding caused a significant increase in final d_H for OVA-HMP system, being this 286 ± 18 nm ($p < 0.05$). However, practically no difference in ζ potential value was observed for OVA-HMP and OVA-RET-HMP systems, suggesting RET binding did not influence on electrical properties of OVA-HMP nanoparticles.

PSD analysis for OVAn and OVAn-RET complexes at pH 4.0 could not be performed due to the gradual particle sedimentation at the bottom of the measurement cell. However, as it can be noted in Fig. 3A, PSD analysis was performed at pH 6.0 yielding the following d_H data: 197 ± 3 nm (98%) and 353 ± 9 nm (96%), for OVAn and OVAn-RET complexes, respectively. Visentini et al. (2016) reported that OVAn is able to bind ~83 RET molecules per OVA monomeric unit in two kinds of RET binding sites, being one of them of higher affinity order (10^5 M^{-1}). Hence, the increased particle size observed for OVAn-RET complexes would be directly linked to the OVAn ability for binding RET. Regarding to the electrical properties of OVAn-RET nanocomplexes, Table 1 shows that RET binding did not modified significantly OVAn ζ potential value ($p > 0.05$), suggesting that colloidal stability of OVAn-RET nanocomplexes is mainly governed by the electrical behaviour of aggregated protein, Following the same procedure described below, BNPs for RET vehiculization were obtained by HMP deposition onto the OVAn-RET nanocomplexes surface. As it was discussed in previous

section, at pH 6.0, the OVAn-HMP system could be characterized by hybrid supramolecular entities or soluble complexes formed through a weak electrostatic interaction between HMP anionic groups and some OVAn cationic surface *patches*. For OVAn-HMP system, a d_H of 231 ± 0 nm (91%) was registered, being this an intermediate size between OVAn (197 ± 3 nm) and HMP ones (990 ± 65 nm). This result support the idea that some level of electrostatic interaction between biopolymers occur in OVAn-HMP system at pH 6.0 (Benichou et al., 2007; Perez, Carrara, Sánchez, Rodríguez Patino, & Santiago, 2009). Besides, this result is supported by the magnitude of ζ potentials, as it can be deduced from Table 1. For OVAn-RET-HMP system, PSD analysis yielded in d_H of 376 ± 10 nm, which was significantly higher than the one registered for OVAn-HMP system ($p < 0.05$). Moreover, it was noted that RET binding practically not alter the OVAn-HMP ζ potential (Table 1).

On the other hand, one question that arises from the analysis of OVAn-HMP systems at pH 6.0, would be if the OVA aggregation (OVAn formation) could be responsible for the observed biopolymer interaction behaviour. To check this hypothesis, PSD and ζ potential for OVA-HMP and OVA-RET-HMP systems were determined at pH 6.0, as it is shown in Fig. 4 and Table 1, respectively. At pH 6.0, a similar PSD behaviour to the one registered at pH 4.0 was observed, registering a first peak at 9 ± 1 nm (94%) and a second one at 52 ± 2 nm (6%). This result could suggest no conformational changes in OVA second and tertiary structure are registered as a consequence of pH changes (Kang, Ryu, Park, Czarnik-Matusewicz, & Jung, 2014). For OVA-RET system, a d_H of 239 ± 0 nm was registered, highlighting the increased particle size as consequence of RET complexation. At pH 6.0, OVA-RET nanocomplexes showed a slight increase in ζ potential value in comparison with pure OVA (Table 1). The same behaviour was found at pH 7.0 (data not shown). For OVA-HMP and OVA-RET-HMP systems, PDS analysis yield the following d_H data: 46 ± 4 nm (88%) and 252 ± 6 nm (96%), respectively, suggesting HMP addition caused a significant increase in OVA and OVA-RET complexes sizes. These findings would indicate the existence of some interactions between biopolymers. However, according to Table 1 for these systems, ζ potential values were −28 ± 1 and −27 ± 1 mV, respectively, which could indicate that electrical properties of these ones are strongly determinated by HMP anionic character (−28 ± 1 mV). Hence, according to these results it could deduce that at pH 6.0, electrostatic interactions in OVA-HMP and OVA-RET-HMP systems would be weaker that the ones observed for OVAn-HMP and OVAn-RET-HMP systems, possible due to HMP net charge was not modified under interaction. So, it is proper to think that OVA aggregation could alter the mode in which biopolymer electrostatically interact at pH 6.0.

In summary, according to PSD and ζ potential results, it can conclude that RET binding promoted a slight increase in d_H, but not alter significantly the BNPs electrical properties, which seemed to be strongly influenced by the HMP anionic character. These findings are in agreement with the ones discussed in the previous section, and in general, they could be linked with the higher colloidal stability observed for these RET vehiculization systems (Lesmes & McClements, 2009; Perez et al., 2015).

3.3. Retinol photochemical stability

It is well known that under certain environmental conditions, light and oxygen promote RET photochemical decomposition by means of formation of inactive species, which adversely affects its bioavailability (Failloux, Bonnet, Perrier, & Baron, 2004). As it was initially mentioned, OVA and OVAn ability for binding RET was reported in Visentini et al. (2016). Moreover from such study, it was elucidated that RET photochemical stability strongly depended on the aqueous medium pH and OVA aggregation state. Nevertheless, hypothesis if polysaccharide addition could improve RET photochemical stability through favorable interactions with OVA and OVAn remained unsolved. This hypothesis was addressed in this section.

The effect of HMP addition on RET photochemical decomposition (%) for OVA-RET (at pH 4.0) and OVAn-RET nanocomplexes (at pH 6.0) is shown in Fig. 5A and B, respectively. Moreover, results for RET photochemical decomposition at 30 h examination and initial DO (mg DO/L) values are reported in Table 2. Firstly, $RET_{darkness}$ and RET_{light} controls should be analyzed. For $RET_{darkness}$ control, it was noted that RET decomposition linearly increased up to 9 h, from which it remain practically constant up to 30 h examination (17.0 ± 1.0%). Hence, result suggest that RET photochemical decomposition due to the DO took place during the first 9 h of testing. In the same way, for RET_{light} control, RET decomposition linearly increased up to 9 h, and then RET decomposition progressed at a lower rate up to reach 33.0 ± 1.0%. For this control, the same DO content should be considered (4.1 ± 0.0 mg DO/L). Therefore, it can suggest that RET decomposition is firstly controlled by DO, and in second place by light. This finding is in agreement with a previous report, highlighting that oxygen

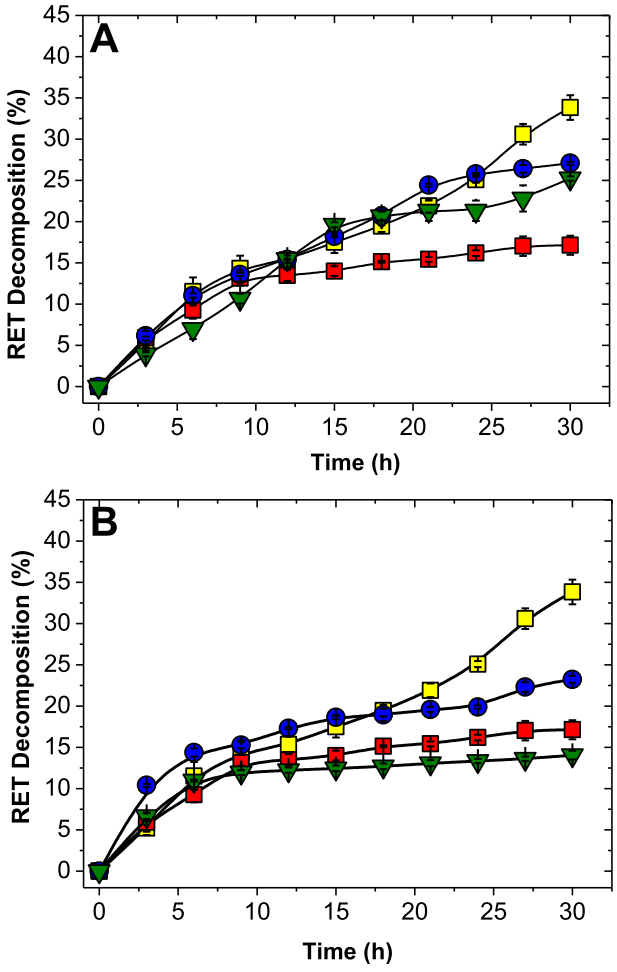

Fig. 5. Retinol (RET) photochemical decomposition (%) as a function of time (h): (A) OVA-RET complex (●) and OVA-RET-HMP complex (▼) at pH 4; (B) OVAn-RET complex (●) and OVAn-RET-HMP complex (▼) at pH 6.0. Controls: (■) pure RET in darkness (RET_{dark}), (▲) pure RET in light (RET_{light}). Conditions: Protein concentration: 6.7 μM (0.028 wt.%), RET concentration: 670 μM, HMP concentration: 0.014 wt.%, Temperature: 25 °C. Experiments were performed using a fluorescent lamp (BAW, 65 W, 750 lm, 6400 K), with exception of RET_{dark} control. Values are showed as mean ± standard deviation.

Table 2
Initial dissolved oxygen concentration (DO mg/L) and retinol (RET) photochemical decomposition (%) at 30 h for 50 mM phosphate buffer, OVA and OVA-HMP pH 4, OVA-HMP, OVAn and OVAn-HMP pH 6. Conditions: Protein concentration: 6.7 μM (0.028 wt.%), RET concentration: 670 μM, HMP concentration: 0.014 wt.%, Temperature: 25 °C.

Systems	RET Decomposition at 30 h (%)	DO (mg DO/L)
$RET_{darkness}$	17.2 ± 1.2^{b}	4.1 ± 0.0^{a}
RET_{light}	33.8 ± 1.5^{f}	4.1 ± 0.0^{a}
OVA-pH 4	27.1 ± 0.2^{e}	3.9 ± 0.1^{a}
OVA-HMP-pH 4	25.0 ± 0.2^{d}	4.6 ± 0.5^{b}
OVA-HMP-pH 6	28.4 ± 1.2^{e}	5.1 ± 0.1^{c}
OVAn-pH 6	23.2 ± 0.4^{c}	$4.3 \pm 0.1^{a,b}$
OVAn-HMP-pH 6	14.1 ± 0.5^{a}	$4.7 \pm 0.3^{b,c}$

Values are showed as mean ± standard deviation and different letters in each column indicate statistical differences ($p < 0.05$).

enhance RET photodegradation (Failloux et al., 2004).

As it can be observed from Fig. 5A, RET decomposition for OVA-RET nanocomplexes at pH 4.0 was quite similar to RET_{light} up to about 24 h, from which take place a RET decomposition less pronounced up to reach 27.1 ± 0.2%. For this system, 3.9 ± 0.1 mg DO/L was registered. This DO content was similar that the one obtained for $RET_{darkness}$ ($p > 0.05$), which would suggest that slight protective effect is mainly due to the OVA-RET complexation.

For OVA-RET-HMP nanoparticle it was noted that RET decomposition was lower than $RET_{darkness}$ up to 9 h analysis, from which it progressed in the same way that RET_{light} until 16 h examination. Then, at the end of testing, a slight decrease in RET decomposition (25.0 ± 0.2%), in comparison with OVA-RET nanocomplex (27.1 ± 0.2%.) was observed. DO determination for OVA-RET-HMP system yielded 4.6 ± 0.5 mg DO/L, being this significantly higher than controls. In spite of this, HMP deposition onto the surface of OVA-RET nanocomplexes would seem to improve slightly the RET protection against DO and light.

On the other hand, as it can de deduced from Fig. 5B, OVAn-RET nanocomplexes at pH 6.0 caused an increase in RET decomposition at short times, suggesting that some RET molecules exposed onto OVAn surface are firstly deteriorated. Then, RET decomposition was similar to RET_{light} control up to 18 h examination, from which a significant reduction in RET decomposition was registered (23.3 ± 0.4%). DO value for this system was 4.1 ± 0.1 mg DO/L, being this similar to the one obtained for $RET_{darkness}$ ($p > 0.05$), suggesting that RET stability could be mainly attributed to the complexation with OVAn. Finally, for OVAn-RET-HMP nanoparticle it was registered that RET decomposition profile was similar to $RET_{darkness}$ control up to 9 h, from which a significant reduction in RET decomposition was registered until 30 h of testing (14.1 ± 0.5%). For this system, 4.7 ± 0.3 mg DO/L was obtained, being this quite higher than the one obtained for the control. Therefore, this finding strongly support the hypothesis that HMP deposition onto OVAn-RET nanocomplex surface significantly improve RET photochemical stability against DO and light. Moreover, at pH 6.0, OVAn-RET-HMP system was more effective than OVA-RET-HMP system for RET photochemical preservation (as it can be deduced from Table 2). This result could be interpreted considering the OVAn particular mode to bind RET and to interact with HMP for BNPs obtention. Furthermore, these OVAn properties would be directly linked with their denatured/aggregated state. It is clearly evident that OVAn-RET-HMP nanocomplexes were the most effective system to preserve RET photochemical stability, which would turn them in promising systems for RET vehiculization in aqueous solution at pH 6.0.

Mixed systems with HMP had higher DO contents than RET controls, which could be explained considering increased oxygen incorporation during systems preparation. As it can be observed in Table 2 and Fig. SM 1 of Supplementary Material, there was not a clear relationship between RET photochemical decomposition and DO concentration, remarking that observed RET protective effect would be mainly attributed to the vehiculization in BNPs.

4. Conclusions

Hypothesis that a polysaccharide deposition onto the protein-RET nanocomplex surface could improve their vehiculization and photochemical stability in aqueous medium was addressed in this work. The assumption was confirmed, highlighting a number of considerations relevant from a practical point of view. Colloidally stable biopolymer nanoparticles (BNPs) for RET delivery can be tailor-made by controlling aqueous medium pH and protein aggregation state. It is worthy to remark that nanosized OVA aggregate can promote BNPs obtention (at pH 6.0) with better properties to vehiculize and to preserve RET in comparison with native OVA. However, BNPs based on native OVA could find suitable applications at pH 4.0. Information derived from this paper could be useful for the development of RET-fortified food formulations and strategies for vehiculization and protection of other sensitive lipophilic compounds.

Acknowledgments

Authors acknowledge the financial support of the following projects: CAI+D-2013-50120110100-171-LI (UNL) and PICT-2014-2636 (ANPCyT), CONICET for the PhD fellowships awarded to Flavia F. Visentini and Osvaldo E. Sponton, and especially to Lic. Alicia Guibert from Centro Universitario Reconquista Avellaneda (UNL, Santa Fe, Argentina) for the kindness of supplying the materials for DO determination.

Appendix A. Supplementary data

Supplementary data related to this article can be found at http://dx.doi.org/10.1016/j.foodhyd.2017.04.020.

References

Benichou, A., Aserin, A., Lutz, R., & Garti, N. (2007). .Formation and characterization of amphiphilic conjugates of whey protein isolate (WPI)/xanthan to improve surface activity. *Food Hydrocolloids, 21*(3), 379–391.

Chanasattru, W., Jones, O. G., Decker, E. A., & McClements, D. J. (2009). Impact of cosolvents on formation and properties of biopolymer nanoparticles formed by heat treatment of β-lactoglobulin–Pectin complexes. *Food Hydrocolloids, 23*(8), 2450–2457.

Chen, L., Remondetto, E. G., & Subirade, M. (2006). Food protein-based materials as nutraceutical delivery systems. *Trends in Food Science & Technology, 17*(5), 272–283.

Cogan, U., Kopelman, S., & Shinitzky, M. (1976). Binding affinities of retinol and related compounds to retinol binding proteins. *European Journal of Biochemistry, 65*(1), 71–78.

Failloux, N., Bonnet, I., Perrier, E., & Baron, M. E. (2004). Effects of light, oxygen and concentration on vitamin A. *Journal of Raman Spectroscopy, 35*, 140–147.

Fioramonti, S. A., Martínez, M. J., Pilosof, A. M. R., Rubiolo, A. C., & Santiago, L. G. (2015). Multilayer emulsions as a strategy for linseed oil microencapsulation: Effect of pH and alginate concentration. *Food Hydrocolloids, 43*, 8–17.

Fioramonti, S. A., Perez, A. A., Aringoli, E., Rubiolo, A. C., & Santiago, L. G. (2014). Design and characterization of soluble biopolymer complexes produced by electrostatic self-assembly of a whey protein isolate and sodium alginate. *Food Hydrocolloids, 35*, 129–136.

Gutiérrez, F. J., Albillos, S. M., Casas-Sanz, E., Cruz, Z., García-Estrada, C., & García-Guerra, A. (2013). Methods for the nanoencapsulation of β-carotene in the food sector. *Trends in Food Science & Technology, 32*, 73–83.

Humblet-Hua, K. N. P., Scheltens, G., van der Linden, E., & Sagis, L. M. C. (2011). Encapsulation systems based on ovalbumin fibrils and high methoxyl pectin. *Food Hydrocolloids, 25*(4), 569–576.

Hunter, R. J. (2001). *Foundations of colloid science* (2nd ed.). New York: Oxford Clarendon Press.

Jones, O. G., & McClements, D. J. (2010). Functional biopolymer Particles: Design,

fabrication, and applications. *Comprehensive Reviews in Food Science and Food Safety, 9*, 374–397.
Joye, I. J., Davidov-Pardo, G., & McClements, D. J. (2014). Nanotechnology for increased micronutrient bioavailability. *Trends in Food Science & Technology, 40*(2), 168–182.
Joye, I. J., & McClements, D. J. (2014). Biopolymer-based nanoparticles and microparticles: Fabrication, characterization, and application. *Current Opinion in Colloid & Interface Science, 19*(5), 417–427.
Kang, D., Ryu, S. R., Park, Y., Czarnik-Matusewicz, B., & Jung, Y. M. (2014). pH-induced structural changes of ovalbumin studied by 2D correlation IR spectroscopy. *Journal of Molecular Structure, 1069*, 299–304.
Lesmes, U., & McClements, D. J. (2009). Structure–function relationships to guide rational design and fabrication of particulate food delivery systems. *Trends in Food Science & Technology, 20*(10), 448–457.
Li, Y., & McClements, D. J. (2013). Influence of non-ionic surfactant on electrostatic complexation of protein-coated oil droplets and ionic biopolymers (alginate and chitosan). *Food Hydrocolloids, 33*(2), 368–375.
Nisbet, A. D., Saundry, R. H., Moir, A. J. G., Fothergill, L. A., & Fothergill, J. E. (1981). The complete amino-acid sequence of hen ovalbumin. *European Journal of Biochemistry, 115*, 335–345.
Noshad, M., Mohebbi, M., Shahidi, F., & Koocheki, A. (2015). Effect of layer-by-layer polyelectrolyte method on encapsulation of vanillin. *International Journal of Biological Macromolecules, 81*, 803–808.
Perez, A. A., Andermatten, R. B., Rubiolo, A. C., & Santiago, L. G. (2014). Beta-lactoglobulin heat-induced aggregates as carriers of polyunsaturated fatty acids. *Food Chemistry, 158*(1), 66–72.
Perez, A. A., Carrara, C. R., Sánchez, C., Rodríguez Patino, J. M., & Santiago, L. G. (2009). Interactions between milk whey protein and polysaccharide in solution. *Food Chemistry, 116*(1), 104–113.
Perez, A. A., Carrera Sánchez, C., Rodríguez Patino, J., Rubiolo, A., & Santiago, L. (2012). Foaming characteristics of β-lactoglobulin as affected by enzymatic hydrolysis and polysaccharide addition: Relationships with the bulk and interfacial properties. *Journal of Food Engineering, 113*(1), 53–60.
Perez, A. A., Sponton, O. E., Andermatten, R. B., Rubiolo, A. C., & Santiago, L. G. (2015). Biopolymer nanoparticles designed for polyunsaturated fatty acid vehiculization: Protein-polysaccharide ratio study. *Food Chemistry, 188*, 543–550.
Qiu, C., Qin, Y., Jiang, S., Liu, C., Xiong, L., & Sun, Q. (2017). Preparation of active polysaccharide-loaded maltodextrin nanoparticles and their stability as a function of ionic strength and pH. *LWT - Food Science and Technology, 76*(A), 164–171.
Rice, E., Baird, R., Eaton, A. D., & Clesceri, L. S. (2012). *Standard Methods for the examination of water and wastewater* (22nd ed.). Washington D.C.: American Public Health Association; American Water Works Association & Water Environment Federation.
Shimoyamada, M., Yoshimura, H., Tomida, K., & Watanabe, K. (1996). Stabilities of bovine β-lactoglobulin/retinol or retinoic acid complexes against tryptic hydrolysis, heating and light-induced oxidation. *Lebensmittel Wissenschaft and Technology, 29*, 763–766.
Sponton, O. E., Perez, A. A., Carrara, C. R., & Santiago, L. G. (2015a). Impact of environment conditions on physicochemical characteristics of ovalbumin heat-induced nanoparticles and on their ability to bind PUFAs. *Food Hydrocolloids, 48*, 165–173.
Sponton, O. E., Perez, A. A., Carrara, C. R., & Santiago, L. G. (2015b). Linoleic acid binding properties of ovalbumin nanoparticles. *Colloids and Surfaces, B: Biointerfaces, 128*, 219–226.
Sponton, O. E., Perez, A. A., Carrara, C. L., & Santiago, L. G. (2016). Complexes between ovalbumin nanoparticles and linoleic acid: Stoichiometric, kinetic and thermodynamic aspects. *Food Chemistry, 211*, 819–826.
Visentini, F. F., Sponton, O. E., Perez, A. A., & Santiago, L. G. (2016). Formation and colloidal stability of ovalbumin-retinol nanocomplexes. *Food Hydrocolloids, 67*, 130–138.
Weijers, M., & Visschers, R. W. (2002). Light scattering study of heat-induced aggregation and gelation of ovalbumin. *Macromolecules, 35*, 4753–4762.
Zeeb, B., Stenger, C., Hinrichs, J., & Weiss, J. (2016). Formation of concentrated particles composed of oppositely charged biopolymers for food applications – impact of processing conditions. *Food Structure, 10*, 10–20.
Zhang, C., Xu, W., Jin, W., Shah, B., Li, Y., & Li, B. (2015). Influence of anionic alginate and cationic chitosan on physicochemical stability and carotenoids bioaccessibility of soy protein isolate-stabilized emulsions. *Food Research International, 77*, 419–425.
Zimet, P., & Livney, Y. D. (2009). Beta-lactoglobulin and its nanocomplexes with pectin as vehicles for ω-3 polyunsaturated fatty acids. *Food Hydrocolloids, 23*, 1120–1126.